Distributed Characterization of Bending-Induced Birefringence in Spun Fibers by means of P-OFDR

Luca Palmieri(1), **Tommy Geisler**(2), **Andrea Galtarossa**(1)

(1) Department of Information Engineering, University of Padova, Via G. Gradenigo 6/B, 35131 Padova, Italy, luca.palmieri@unipd.it, andrea.galtarossa@unipd.it

(2) OFS Fitel Denmark ApS, Priorparken 680, 2605 Brøndby, Denmark, tgeisler@ofsoptics.com

Abstract: We report, for the first time, spatially-resolved measurements of bending-induced birefringence in ad hoc drawn single-mode spun fibers. The combined effect of spin rotation and bending birefringence is clearly highlighted.

OCIS codes: (060.2270) Fiber characterization, (060.2300) Fiber measurements.

The birefringence caused by asymmetries and perturbations in single-mode optical fibers is known to be the origin of PMD [1]. Because of this, birefringence has been the subject of extensive theoretical and experimental analyses, that date back more than thirty years [2–4].

Among the techniques exploited to investigate fiber birefringence, polarization-sensitive reflectometry (PSR) proved quite effective. This technique may be implemented either in the time domain (P-OTDR) [5] or in the frequency domain (P-OFDR) [6–8], but in both cases it is based on the analysis of the polarization state (SOP) of the field backscattered by the fiber as a probe field propagates in it. Actually, the evolution of the backscattered SOP as a function of distance is related to the fiber local birefringence; hence, to measure the former may yield information on the latter, provided that raw data are accurately processed. In this respect, it has been recently shown that PSR can indeed provide an almost complete point-wise characterization of fiber birefringence, the only limitation being an intrinsic inability in distinguishing linear birefringence rotation from circular birefringence [8].[†]

In the present paper, we report P-OFDR measurements of bending-induced birefringence in ad hoc drawn spun fibers. Although several papers have been already dedicated to bending-birefringence [4,9], to the best of our knowledge this is the first time that a distributed, point-wise measurement of bending-birefringence is performed and reported. Actually, owing to the high spatial resolution of the P-OFDR and to the accuracy of the data analysis algorithm, we have been able to record the local variation of the birefringence vector along fiber samples part of which were wound in small loops. This experiment has been performed on spun fibers because the spin imparts to the birefringence an ordered structure, easily recognizable in the measurements.

As anticipated above, reflectometric measurement of birefringence is based on the analysis of the backscattered field. Actually, its SOP, $\hat{s}_B(z)$, is governed by the equation $d\hat{s}_B/dz = \bar{\beta}_B(z) \times \hat{s}_B(z)$, where $\bar{\beta}_B(z) = 2\boldsymbol{M}\boldsymbol{F}^T(z)\bar{\beta}_A(z)$ is the round-trip birefringence, $\boldsymbol{M} = \mathrm{diag}(1,\,1,\,-1)$ is a diagonal matrix and $\boldsymbol{F}(z)$ is the Mueller matrix representing propagation from the fiber input up to z. The vector $\bar{\beta}_A(z)$ is the "apparent" birefringence seen by the reflectometric measurement and is related to the "real" local birefringence of the fiber. In its most general form, this relationship may be written as $\bar{\beta}_A(z) = \boldsymbol{R}_3\big[-g\tau(z)\big]\bar{\beta}_L(z)$, where: $\bar{\beta}_L(z) = \beta_L(z)(\cos 2\psi(z),\, \sin 2\psi(z),\, 0)^T$ is the linear component of the fiber "real" birefringence; $\psi(z) = \eta(z) + A(z) + \tau(z)$; $\eta(z)$ is the birefringence intrinsic orientation (usually random); $A(z)$ and $\tau(z)$ are the rotations (possibly) imparted by spin and twist, respectively, and $\boldsymbol{R}_3(\phi)$ is a rotation by an angle ϕ around the $\hat{s}_3 = (0,\,0,\,1)^T$ axis [8]. Note that the circular birefringence caused by the twist enters in the expression of $\bar{\beta}_A(z)$ as an apparent rotation $\boldsymbol{R}_3[-g\tau(z)]$, $g \simeq 0.144$ being the torsional stress coefficient [10].

By measuring $\hat{s}_B(z)$ it is possible to calculate the round-trip birefringence $\bar{\beta}_B(z)$. Afterwards, $\boldsymbol{F}(z)$ can be calculated by solving the differential equation $d\boldsymbol{F}/dz = (\boldsymbol{M}\bar{\beta}_B/2) \times \boldsymbol{F}$, $\boldsymbol{F}(0) = \boldsymbol{I}$, and, finally, $\bar{\beta}_A(z)$ can be determined as $\bar{\beta}_A(z) = (1/2)\boldsymbol{F}(z)\boldsymbol{M}\bar{\beta}_B(z)$ [8]. We remark that $\bar{\beta}_A(z)$ represents the most complete information about fiber birefringence that can be retrieved via PSR.

It is worthwhile analyzing more in detail what happens when a twisted fiber is coiled. As well known, the winding induces a linear birefringence whose optical axes are parallel and orthogonal to the curvature

[†]This limitation may be however overridden by preparing the experiment properly or by repeating the measurement under different, controlled conditions.

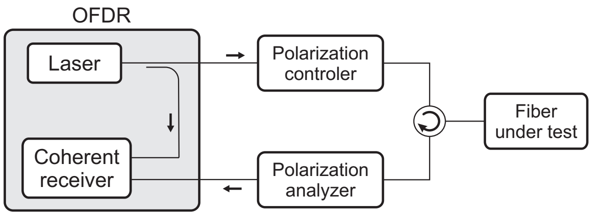

Fig. 1. Schematic of the experimental set-up.

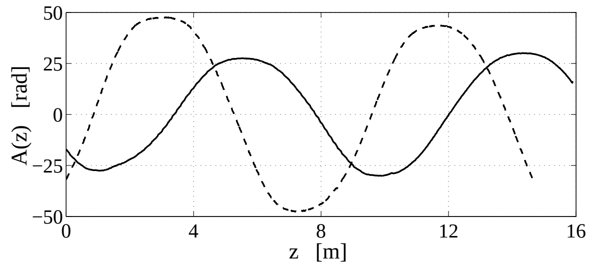

Fig. 2. Spin profiles of samples A (solid) and B (dashed).

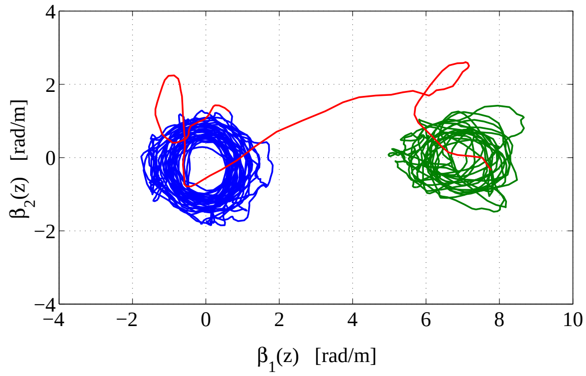

Fig. 3. Parametric plot of the birefringence measured on sample A. Blue and green: fiber sections wound on 180 mm and 34.5 mm diameters, respectively. Red: fiber section connecting the two previous ones.

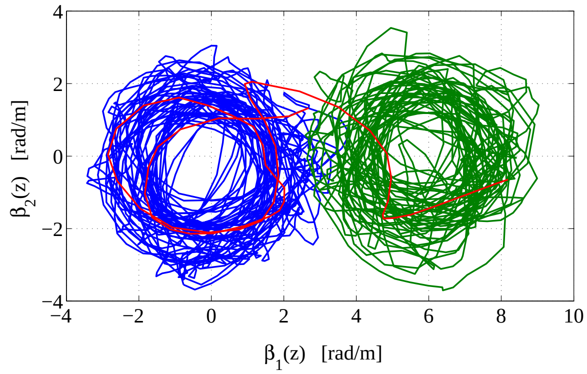

Fig. 4. Parametric plot of the birefringence measured on sample B. Blue and green: fiber sections wound on 180 mm and 38.0 mm diameters, respectively. Red: fiber section connecting the two previous ones.

plane and whose modulus (at 1550 nm) is $\beta_W \simeq 5.49 \times 10^7 (r/R)^2$ rad/m, where $r = 62.5$ μm is the fiber radius and R is the bending one [4]. Therefore, if the fiber is wound with a constant radius in tight loops, the induced birefringence vector, $\bar{\beta}_W$, is constant. In the limits of validity of the coupled-mode theory, the winding-induced birefringence adds to the intrinsic one, $\bar{\beta}(z)$, giving a total birefringence $\bar{\beta}_T(z) = \bar{\beta}(z) + \bar{\beta}_W$.

Note that if any twist is affecting the fiber, this would affect only $\bar{\beta}(z)$ and not $\bar{\beta}_W$, whose direction is related only to the winding plane. Nevertheless, if a reflectometric measurement is performed, the resulting apparent birefringence would be $\bar{\beta}_A(z) = \boldsymbol{R}_3[-g\tau(z)](\bar{\beta}_L(z) + \bar{\beta}_W)$, which means that also the winding birefringence is seen to rotate, as a consequence of the circular birefringence affecting the fiber. For this reason, particular care should be taken to avoid any twist when measuring the bending induced birefringence.

To verify the effects of winding on fiber birefringence, we have performed P-OFDR measurements on two samples of spun fibers, coiled with different radii. The experimental setup, schematically shown in fig. 1, consists of an OFDR modified to allow the control of the probe-field SOP and the polarization analysis of the backscattered one [8].

Measurements have been performed on two ad hoc drawn spun fibers, whose spin profiles, $A(z)$, have been characterized with the technique reported in [8]; results are shown in fig. 2. Both fibers have about the same spin period of 8.6 m, whereas the peak-to-peak spin amplitudes are different: about 60 rad the first fiber (sample A, solid curve) and about 90 rad for the the second one (sample B, dashed curve). The two samples have also different birefringence strength, as they have been drawn from two different preforms; actually, the beat length, L_B, is about 5.1 m for sample A and 2.7 m for samples B. Bending characterization has been performed on fiber spans of about 15 m. Half of the span was wound on a standard shipping bobbin (diameter 180 mm) while the other half was wound around cylinders with diameters ranging from 34.5 mm up to 80 mm. As explained before, the winding was done putting extreme care to avoid any twist.

Fig. 3 shows the parametric plot of the two components of the birefringence measured on sample A. The blue portion of the curve refers to the sample section wound on the shipping bobbin: the ring-shape is due to the rotation imparted by the spin, whereas the thickness is caused mainly by the variation of birefringence strength and partly by noise. Notice that this ring is not perfectly centered on the axes origin because of the tiny amount of bending birefringence induced by the winding on the bobbin. The green portion of the curve

OWS2.pdf

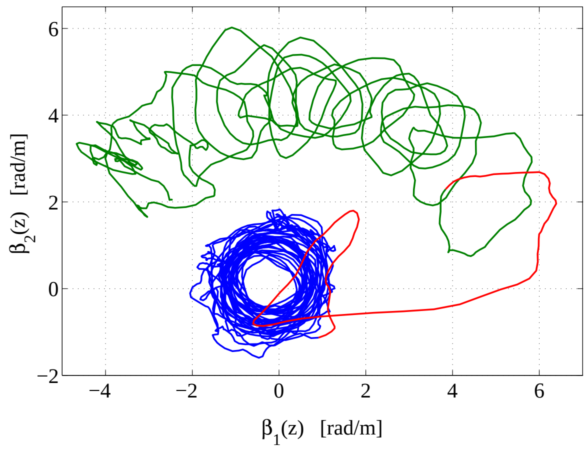

Fig. 5. Parametric plot of the birefringence measured on sample A when this is affected by twist.

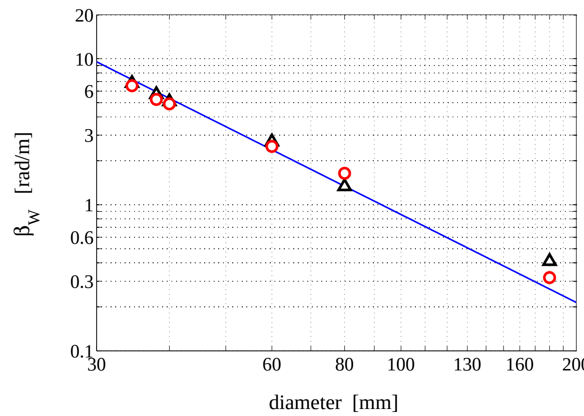

Fig. 6. Bending-birefringence vs. bending diameter. Circles: sample A; triangles: sample B; line: theory [4].

refers to the section of fiber wound on a diameter of 34.5 mm. Clearly, this winding has induced a strong and almost constant birefringence, that has moved the ring away from the axes origin. We may also note that, in this section, the ring is not as well marked as in the previous one; likely, this is due to some residual twist and to a small non-constant birefringence accidentally induced during the winding (which was done by hand and hence lacked a control of the winding tension [9]). Finally, the red portion of the curve refers to the section of fiber connecting the two previous ones. Similar results have been obtained using sample B, as shown in fig. 4. The colors have the same meaning as before, with the only difference that the green portion refers to a section wound on a diameter of 38.0 mm. In this case, the rings are wider because sample B has a higher intrinsic birefringence; for the same reason, the fiber is less sensitive to external perturbation and hence the green loop, differently from sample A, is still well marked. Fig. 5 shows the effects of twist (sample A; diameter 40 mm; colors as before). As explained above, the twist-induced circular birefringence causes an apparent rotation of bending-birefringence. This rotation, combined with the one due to the spin, originates the sort of epicycloid shown by the green section of the curve.

The rings shown in figs. 3 and 4 can be used to estimate the modulus of the winding-induced birefringence, β_W. Actually, this modulus is just the distance of the ring centers from the axes origin. The winding-induced birefringence has been estimated in this way for different winding radii. Results are shown in fig. 6 and are in good agreement with the theoretical prediction [4].

In conclusion, we have reported, for the first time to the best of our knowledge, a distributed, point-wise characterization of bending-induced birefringence. The measurements have clearly shown the interplay between bending, spin and twist and have confirmed that high-resolution PSR is an effective tool for birefringence characterization.

Partial support from the Italian Ministry of Foreign Affairs (Direzione Generale per la Promozione e la Cooperazione Culturale) is acknowledged.

References

[1] A. Galtarossa, C. R. Menyuk Eds., *Polarization Mode Dispersion.* New York: Springer, 2005.
[2] A. Simon, R. Ulrich, "Evolution of polarization along a single-mode fiber," *Appl. Phys. Lett.*, **31**, 517–520, 1977.
[3] S. C. Rashleigh, "Origins and control of polarization effect in single-mode fibers," *J. Lightwave Technol.*, **1**, 312–331, 1983.
[4] R. Ulrich, S. C. Rashleigh, W. Eickhoff, "Bending birefringence in single-mode fibers," *Opt. Lett.*, **5**, 273–275, 1980.
[5] A. Galtarossa, L. Palmieri, "Spatially resolved PMD measurements," *J. Lightwave Technol.*, **22**, 1103–1115, 2004.
[6] M. Wegmuller, M. Legré, N. Gisin, "Distributed beatlength measurement in single-mode fibers with optical frequency-domain reflectometry," *J. Lightwave Technol.*, **20**, 828–835, 2002.
[7] T. Geisler, P. Kristensen, O. Knop, "New details of spun fibers measured with an OFDR," *Tech Digest. OFC (paper OWA3)*, Anaheim (CA), 2006.
[8] A. Galtarossa, D. Grosso, L. Palmieri, M. Rizzo, "Spin-profile characterization in randomly birefringent spun fibers by means of frequency-domain reflectometry," *Opt. Lett.*, **34**, 1078–1080, 2009.
[9] S. C. Rashleigh, R. Ulrich, "High birefringence in tension-coiled single-mode fibers," *Opt. Lett.*, **5**, 354–356, 1980.
[10] A. Galtarossa, D. Grosso, L. Palmieri, L. Schenato, "Reflectometric measurement of strain induced optical activity coefficient in single-mode randomly birefringent twisted fibers," *35th ECOC*, Wien (A), 2009.